

Oxaphosphetane versus betaine formation in epoxide ring opening by PPh_3 : a mechanistic probe by ab initio and DFT modeling

Anbarasan Kalaiselvan and Ponnambalam Venuvanalingam*

School of Chemistry, Bharathidasan University, Tiruchirappalli 620 024, India

Received 3 February 2005; revised 28 March 2005; accepted 5 April 2005

Available online 22 April 2005

Abstract—Ab initio and density functional investigations on the deoxygenation of *cis*-2,3-dimethylepoxyde by PPh_3 reveal a two-step mechanism. Simultaneous ring-opening and C–C bond rotation facilitates oxaphosphetane formation thereby ruling out the formation of a betaine intermediate and is consistent with the inversion of stereochemistry observed in the reaction.

© 2005 Elsevier Ltd. All rights reserved.

The Wittig¹ reaction is an important organic transformation. The ring-opening of epoxides by triphenylphosphine is a versatile tool for the inversion of olefin stereochemistry. In spite of its importance in organic synthesis, the mechanism of the Wittig reaction has been the subject of debate for a long time.² In particular, it is not clear if the reaction passes through a betaine-type intermediate or not. In some cases, the betaine type intermediate has been isolated as a lithium salt and not as a true betaine.³ Vedejs⁴ has argued that the reaction passes through a four-centered TS leading directly to an oxaphosphetane (OP) and not through a betaine. The question of formation of an oxaphosphetane as an intermediate directly or via a betaine-type intermediate has been investigated by several workers⁵ both experimentally and theoretically, although there is no clear answer. Oxaphosphetane intermediates are highly unstable and readily breakdown to an alkene and phosphine oxide either through a concerted or stepwise mode. Earlier studies report that oxaphosphetanes decompose through either of these modes.^{2,4–6} Epoxide ring opening with tri-substituted phosphines occurs only at elevated temperatures.⁷

The above situations have stimulated us to explore the mechanism of the cleavage of *cis*-2,3-dimethylepoxyde

with PPh_3 with the following questions in mind; (i) Whether betaine formation precedes the oxaphosphetane formation? (ii) Whether the decomposition of the oxaphosphetane is concerted or stepwise? (iii) How does the mechanism explain the inversion of stereochemistry?

Geometry optimizations were carried out using a density functional approach with the B3LYP functional⁸ and with the HF⁹ method using the 6-31G(d) basis set.¹⁰ All stationary points located were characterized by computing vibrational frequencies. TSs were confirmed by harmonic analysis and by IRC.¹¹ Further single point energy calculations were performed at B3LYP and MP2 levels, respectively with 6-311++G(d,p) and 6-31G(d) basis sets on B3LYP/6-31G(d) optimized geometries. The free energies of the species at HF and B3LYP levels with the 6-31G(d) basis set were calculated based on thermo-chemical calculations and single point free energy calculations were performed using thermal correction data obtained at the B3LYP/6-31G(d) level. Bond orders reported here are Wiberg¹² bond indices calculated using the Natural Bond Orbital (NBO) program.¹³ From these bond orders, bond formation and cleavage indices were calculated as reported earlier.¹⁴ A bond formation-cleavage average index for the P1–C35 bond was calculated by giving 50% weight to formation and 50% weight to cleavage, since this bond forms fully in the intermediate and is cleaved totally at the end of the reaction. All calculations were performed using the Gaussian 98W program.¹⁵

Keywords: Deoxygenation; Ab initio and DFT modeling; Oxaphosphetane; Betaine.

* Corresponding author. Tel.: +91 4312407053; fax: +91 4312407045; e-mail: venuvanalingam@yahoo.com

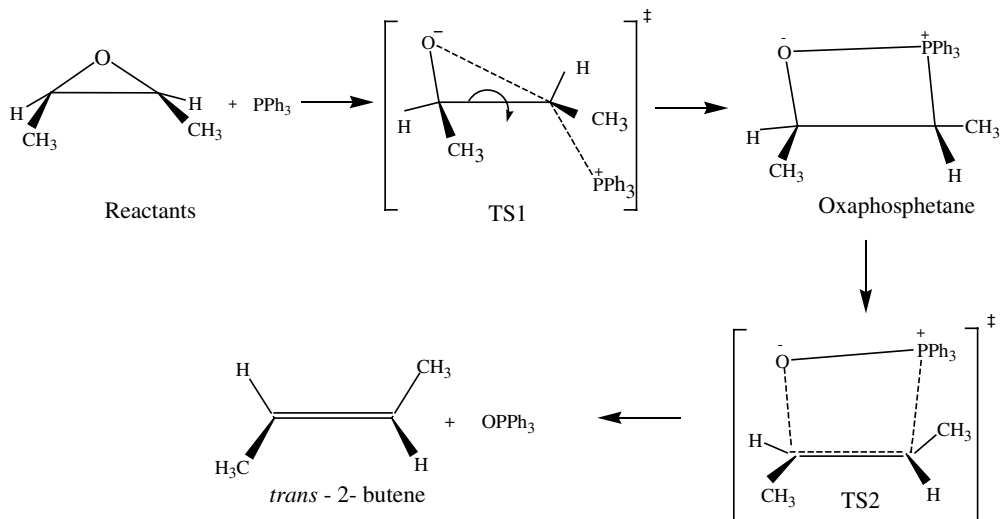


Figure 1. Reaction pathway for the deoxygenation of *cis*-2,3-dimethylepoxyde with PPh_3 .

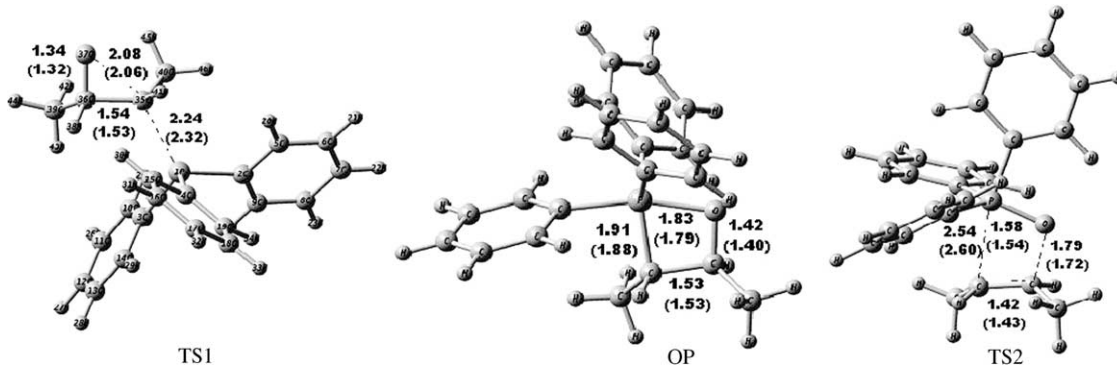


Figure 2. Optimized structures of the transition states and intermediate OP in the deoxygenation of the *cis*-epoxide with triphenylphosphine at the B3LYP/6-31G(d) level. Distances are in Å.

The detailed reaction scheme is given in Figure 1. Optimized geometries for the species in the reaction pathway are presented in Figure 2.

Triphenylphosphine approaches the epoxide carbon from behind the ring to form TS1 transferring a charge of -0.4 . In this transition state, the P1-C35 bond is partially formed and the C35-O37 bond sharing the same carbon atom is partially cleaved. Intrinsic Reaction Coordinate analysis explains very well the geometrical changes along the reaction pathway (Fig. 3a) as follows. From TS1, along the reaction coordinate, the dihedral angle $\langle \text{P1}-\text{C35}-\text{C36}-\text{O37} \rangle$ is gradually changed from 163.2° to 18.3° while the C35-O37 bond is breaking and the P1-C35 bond is forming. Rotation of the C35-C36 bond pushes the methyl group attached to the reacting carbon to adopt a *trans* orientation. Another interesting feature is that during this C35-C36 bond rotation, first the C-C bond lengthens up to 1.73 \AA and then it reduces, finally to 1.54 \AA . The simultaneous rotation of the C-C bond and ring opening of the epoxide along the reaction path results in oxaphosphetane formation directly and clearly rules out the formation of a betaine intermediate. The observations are in good agreement with earlier experimental reports of

the Wittig reaction involving aldehydes and phosphonium ylides and that OP formation is essentially a concerted process.^{2,6} In the OP, the four atoms P1, C35, C36, and O37 are in a slightly distorted coplanar state where the phosphorus atom is in a trigonal bipyramidal coordination in which the oxygen atom is in the axial position as reported by Hoffmann et al.¹⁶ The P1-O37 bond length observed is somewhat larger in the OP,¹⁷ that is, it is weak due to the large steric hindrance due to the three phenyl substituents on phosphorus.

In the second step, the OP undergoes decomposition through TS2 in a concerted asynchronous manner with P1-C35 bond breaking to form *trans*-2-butene and Ph_3PO . Changes in the P1-C35 and C36-O37 bond lengths along the IRC for the second step clearly show that cleavage of the P1-C35 bond occurs well ahead of C36-O37 bond cleavage (Fig. 3b).

The relative free energies of the species listed in Table 1 show that the barrier for the ring opening step is $52.9 \text{ kcal mol}^{-1}$. Here the C35-O37 bond is cleaved well ahead of P1-C35 bond formation and this results in a higher activation energy. The higher activation barrier for step 1 agrees well with the experimental observation

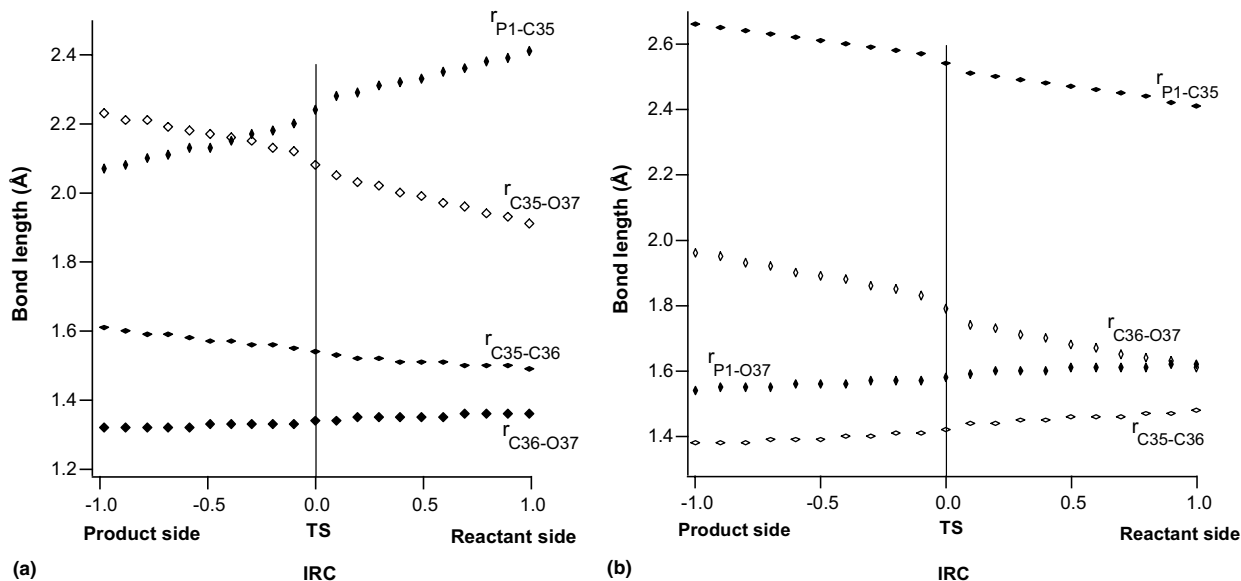


Figure 3. Changes in the lengths of various bonds along the IRC around (a) TS1, (b) TS2. The units of IRC are $\text{amu}^{-1/2}$ Bohr.

Table 1. Relative free energies (kcal mol^{-1}) of TSs, intermediate and products for the deoxygenation of *cis*-2,3-dimethylepoxyde at various computational methods relative to the reactants

Method	TS1	OP	TS2	Products
HF/6-31G(d)	69.9	26.5	50.4	–36.3
B3LYP/6-31G(d)	52.9	16.6	35.1	–32.0
B3LYP/6-31++G(d,p) ^a	50.0	20.5	37.6	–32.1
MP2/6-31G(d) ^a	51.7	1.3	24.6	–33.3

^a Values obtained with single point calculations at the specified level on the B3LYP/6-31G(d) geometries.

that this reaction requires high temperatures.⁷ Computed deformation energies (epoxide 47.9 kcal mol^{-1} and $\text{PPh}_3 = 2.1 \text{ kcal mol}^{-1}$) show that the epoxide has to distort to a greater extent to form TS1 and this increases the activation energy for the first step.

HF/6-31G(d) free energies are higher while at other barriers (Table 1) they are lower. MP2/6-31G(d) free energies are lower when compared to B3LYP/6-31G(d) values. The free energies listed in Table 1 suggest that step 1 is rate determining. The higher exothermicity observed here is due to the release of ring strain. The calculated bond indices in Table 2 show that bond formation and cleavage take place systematically and the gradual increase in BFC_{Ave} values from reactants

to products explains the progress of the reaction quantitatively.

Deoxygenation of *cis*-2,3-dimethylepoxyde using PPh_3 results in the formation of dimethyl alkenes with inversion of stereochemistry. Calculations reveal that the reaction takes place in two steps. (1) In the first step, PPh_3 attacks from behind the epoxide carbon and results in oxaphosphetane formation. Simultaneous ring opening and C–C bond rotation lead to formation of the oxaphosphetane and rule out the intermediacy of a beta-ine. (2) This oxaphosphetane undergoes asynchronous concerted cycloreversion to form the inverted alkene. C–C bond rotation and concerted cleavage of the oxaphosphetane lead to inversion of the stereochemistry

Table 2. Wiberg bond order analysis of the deoxygenation of *cis*-2,3-dimethylepoxyde with triphenylphosphine

Species	Bond formation			Bond cleavage		$\text{BFC}_{\text{Ave}}^{\text{a}}$
	C35–C36	P1–C35	P1–O37	C35–O37	C36–O37	
Reactants	0.0	0.0	0.0	0.0	0.0	0.0
TS1	0.0	36.3	0.0	63.3	0.0	19.9
Oxaphosphetane	0.0	50.0	38.0	100.0	0.0	37.6
TS2	35.1	85.0	72.7	100.0	47.5	68.1
Products	100.0	100.0	100.0	100.0	100.0	100.0

^a BFC_{Ave} is the average percentage of all bond forming and cleaving indices of various species in the reaction step (see Ref. 14).

consistent with the experimental reports. The computed bond indices describe the bond formation and cleavage process during the reaction very well.

Acknowledgements

The financial assistance from UGC, India through Major Research Grant No. F.12-30/2002 (SR-1) Dt 21st May 2002 is gratefully acknowledged.

Supplementary data

HF/6-31G(d), B3LYP/6-31G(d) optimized Cartesian coordinates of the species in the reaction path. Geometrical changes from TS1 to OP are shown in Fig S1. Supplementary data associated with this article can be found, in the online version at doi:10.1016/j.tetlet.2005.04.024.

References and notes

1. Wittig, G.; Hagg, W. *Chem. Ber.* **1955**, *88*, 1654.
2. Holler, R.; Lischka, H. *J. Am. Chem. Soc.* **1980**, *102*, 4632.
3. Vedejs, E.; Meier, G. P.; Snoble, K. A. *J. Am. Chem. Soc.* **1981**, *103*, 2823.
4. Vedejs, E.; Marth, C. F. *J. Am. Chem. Soc.* **1988**, *110*, 3948.
5. (a) Maryanoff, B. E.; Reitz, A. B. *Chem. Rev.* **1989**, *89*, 863; (b) Maercker, A. *Org. React.* **1965**, *14*, 270; (c) Bestmann, H. J. *Pure Appl. Chem.* **1980**, *52*, 771; (d) Volatron, F.; Eisentein, O. *J. Am. Chem. Soc.* **1987**, *109*, 1; (e) Volatron, F.; Eisentein, O. *J. Am. Chem. Soc.* **1984**, *106*, 6117.
6. Bestmann, H. J. *Pure Appl. Chem.* **1979**, *51*, 515.
7. (a) Vedejs, E.; Fuchs, P. L. *J. Am. Chem. Soc.* **1971**, *93*, 4030; (b) Vedejs, E.; Fuchs, P. L. *J. Am. Chem. Soc.* **1973**, *95*, 822.
8. (a) Becke, A. D. *J. Chem. Phys.* **1993**, *98*, 5648; (b) Lee, C.; Yang, W.; Parr, R. G. *Phys. Rev. B* **1988**, *37*, 785.
9. Roothaan, C. C. *J. Rev. Mod. Phys.* **1951**, *23*, 69.
10. Frisch, M. J.; Pople, J. A.; Binkley, J. S. *J. Chem. Phys.* **1984**, *80*, 3265.
11. (a) Fukui, K. *J. Phys. Chem.* **1970**, *74*, 4161; (b) Ishida, K.; Morokuma, K.; Komornicki, A. *J. Chem. Phys.* **1977**, *66*, 2153.
12. Wiberg, K. *Tetrahedron* **1968**, *24*, 1083.
13. (a) Reed, A. E.; Curtiss, L. A.; Weinhold, F. *Chem. Rev.* **1988**, *88*, 889; (b) Foster, J. P.; Weinhold, F. *J. Am. Chem. Soc.* **1980**, *102*, 7211.
14. Kalaiselvan, A.; Venuvanalingam, P.; Poater, J.; Solà, M. *Int. J. Quant. Chem.* **2005**, *102*, 139.
15. *GAUSSIAN* 98 (Revision A.9), Gaussian Inc., Pittsburgh, PA, **1998**.
16. Hoffmann, R.; Howell, J. M.; Muetterties, E. L. *J. Am. Chem. Soc.* **1972**, *94*, 567.
17. (a) Yamataka, H.; Hanafusa, T.; Nagase, S.; Kurakake, T. *Heteroatom Chem.* **1991**, *2*, 465; (b) Yamataka, H.; Nagase, S. *J. Am. Chem. Soc.* **1998**, *120*, 7530.